Biol. Cybern. 64, 263–272 (1991)

Biological Cybernetics

Theory of ocular dominance column formation

Mathematical basis and computer simulation

Shigeru Tanaka

Fundamental Research Laboratories, NEC Corporation 34 Miyukigaoka, Tsukuba, Ibaraki, 305 Japan and
Laboratory for Neural Networks, RIKEN Frontier Research Program, Hirosawa 2-1, Wako, Saitama, 351-01 Japan

Received May 7, 1990/Accepted in revised form September 15, 1990

Abstract. A general theory previously proposed by the author which describes synaptic stabilization on the basis of three basic assumptions is employed for the understanding of ocular dominance column formation. A reduced mathematical model is constructed based on the thermodynamics in the Ising spin variables representing the afferent synaptic connection distribution. The results of Monte Carlo simulations on the segregation of ipsilateral and contralateral synaptic terminals in the input layer of the primary visual cortex suggest the existence of phase transition phenomena. Three types of ocular dominance column patterns – stripe, blob, and uniform – are visualized according to the values of the correlation strength and the degree of imbalance in activity between the left and right retinas. The theory presented here successfully explains how ocular dominance columns are developed.

1 Introduction

The cerebral cortex has characteristic map structures such as ocular dominance columns (ODC) (Hubel and Wiesel 1977), orientation columns (Hubel et al. 1978), color-specific blobs (Livingstone and Hubel 1984), frequency columns (Knudsen et al. 1987), and somatosensory patches (Kaas et al. 1983). These structures, often called functional architecture (Hubel and Wiesel 1977), are important examples of the functional-structural relationship of the brain. Recent experiments have shown that these specific structures are constructed in an activity-dependent manner (Frank 1987). For example, abnormal ODCs were formed in cats and monkeys reared under unusual visual conditions (e.g., Hubel et al. 1977). Apparently, neuronal activity elicited by external stimuli plays a role in the morphogenesis of the nervous system.

Mechanisms of self-organization of the ODC have been a subject of theoretical investigations. Swindale (1980) has pointed out that competition between short-range intracortical excitation and long-range intracortical inhibition leads to a stripe pattern similar to the monkey ODC pattern (Hubel and Wiesel 1977). Von der Malsburg (1979) and Miller et al. (1989) showed that a coincidence of pre- and postsynaptic activities – the Hebbian mechanism of synaptic plasticity – successfully describes activity-dependent self-organization of the ODC stripe pattern. These models, however, include an additional arbitrary constraint to avoid divergence in synaptic strength or synaptic efficacy (Miller et al. 1989; Linsker 1986). Therefore, we may say that these models are practical and empirical. If we want to build a model which systematically explains the accumulated experimental data concerning visual deprivation, pharmacological effects, and the results of comparative studies, we must adopt mathematical parameters which have biological counterparts. For this sake, the mathematical description should be derived from a small number of basic assumptions which have clear biological meanings.

Recently, the author proposed a general theory of activity-dependent self-organization of cortical maps using the thermodynamics in the spin system described by the Hamiltonian (Tanaka 1988, 1989, 1990a). Parameters involved in this theory can be related to biological factors since the theory is built on the basis of hypothetical mechanisms of synaptic stabilization due to *(1)* a postsynaptic factor released from dendrites of a target cell. *(2)* a presynaptic factor transported from the presynaptic cell body, and *(3)* a Hebb-like coincidence of pre- and postsynaptic activities. The thermodynamic formulation of this general theory enables us to perform both mathematical calculations and computer simulations according to the conventional methods of thermodynamics without the introduction of any additional constraint. Also, the obtained theoretical results can be easily compared with experimental data since the parameters used in this theory can be interpreted biologically.

This report is the first of a series of papers which will describe ODC formation on the basis of the general

theory. A reduced mathematical model specific to ODC formation will be derived, and computer simulations based on this model will reproduce physiological features of ODC segregation in the old-world monkey. Three basic parameters will be introduced. One is the correlation strength in activity between the left and right retinal ganglion cells (RGC), another is the degree of imbalance in activity between them, and the other is the effective temperature. It will be shown that weak activity correlation between the left and right retinas is essential to ODC segregation, and that the effective temperature regulates the segregation process. It will also be shown that imbalanced activities between the left and right retinas yield asymmetric stripe patterns or blob patterns. Moreover, the occurrence of hysteresis between these two types of patterns will be predicted.

2 Basic mechanisms

We follow Changeux and Danchin's (1976) hypothesis which proposes that at least three states for the synapse exist: labile, stable, and regressed. The labile and stable states are capable of transmitting electrical activity, but the regressed state is not. The synaptic modification corresponds to mutual transition among these three states. Hereafter, we shall refer to the transition from the labile state to the stable state as stabilization, and the opposite transition as destabilization. The hypothesis further claims that it is possible for the labile state either to reach the stable state or to degrade into the regressed state. However, our theory will not give an explicit mathematical description of the latter possibility, as we assume that only the stable synapses will remain after the so-called critical period.

The author postulates three mechanisms (Tanaka 1989, 1990a) underlying the activity-dependent self-organization of neural connections as follows: *(1)* modifiable synapses are stabilized due to a limited amount of a postsynaptic factor released from dendrites of a target cell per unit time; *(2)* the stability of the synapses is also regulated by a presynaptic factor which is synthesized in a presynaptic cell body and transported through the axon to presynaptic terminals; *(3)* furthermore, the synaptic stabilization obeys a local rule of Hebbian type; if the presynaptic spike activity coincides with postsynaptic local membrane depolarization (hyperpolarization), the synapses are stabilized (destabilized). The following physiological meanings may be attached to the postulated three mechanisms.

Mechanism *(1)* leads to the competition among synapses for the limited amount of the postsynaptic factor which is secreted from the target neurons. If there is a small number of synapses within a region whose size is determined by the diffusion length of the factor, each synapse takes a sufficient amount of the factor to stabilize. On the other hand, if there is a large number of synapses within the region, the amount of the factor which one neuron can take decreases. Therefore, the density of stable synaptic connections is likely to be constant. Furthermore, this mechanism together with mechanism *(3)* gives rise to a winner-take-all process.

Mechanism *(2)* describes stabilization by the presynaptic factor which is synthesized in cell bodies in the presynaptic layer and sent through their axons to terminals in the target layer. Owing to this mechanism, the synapses which have once been destabilized to the labile state can come to be stabilized again. This type of stabilization is independent of any postsynaptic event. It is thought that the synaptic stabilization attributed to the presynaptic factor occurs only within a limited region in which terminals of the axon from the presynaptic cell body arborize because the factor cannot be transported to the outside of this region. The time course for the stabilization process is determined by the amount of the presynaptic factor secretion; the stabilization process takes longer if a small amount of this factor is available, while it is shorter in the opposite case. The detailed mathematical analysis (Tanaka 1990a) shows that this time course determines the effective temperature as described in (A1.3). Thus, finite temperature effects, if any, can be attributed to the presynaptic factor secretion.

Mechanism *(3)* implies that if the neurotransmitter is released from the presynaptic side simultaneously with the occurrence of the postsynaptic membrane depolarization, then the synapse receives a reward which promotes its stabilization. On the other hand, if the release of the neurotransmitter and the postsynaptic membrane hyperpolarization takes place simultaneously, a penalty is imposed on the synapse, causing it to destabilize. This hypothetical mechanism is the likeliest model for explaining experimentally observed synaptic plasticity (Collingridge and Bliss 1987).

3 Model Hamiltonian

In the first place, we will discuss approximations employed in reducing the general Hamiltonian to the one specific to ODC formation.

It is natural to think that retinotopic order is also developed in an activity-dependent manner during ODC formation. Therefore, we should consider both types of development at the same time. In the present paper, however, we assume that retinotopic order is already completed and well defined before ODC formation begins. Although this assumption appears unrealistic, we can simplify the problem significantly and thereby obtain essential features of ODC formation. From another preliminary result of computer simulations in which the development of retinotopic order is taken into account at the same time, the author has confirmed that the degree of freedom of retinotopy does not have much qualitative effect on ODC segregation (Tanaka 1990b). Submodalities other than ocular dominance, such as on-centre or off-centre, color-specific or color-nonspecific, and magnocellular or parvocellular pathways will not be considered, either.

The detailed derivation of an appropriate Hamiltonian H which describes ODC formation will be dis-

cussed in Appendix 2. This Hamiltonian is given by the following form:

$$H = -h\sum_j s_j - \frac{J}{2}\sum_{j\neq j'}\sum_{j'} U_{j,j'}s_j s_{j'} . \tag{3.1}$$

The parameters J and h are written in terms of the correlation strength between the left and right RGC firings and the degree of imbalance in firing activity between the left and right RGCs (Let r and α denote the correlation strength and the degree of imbalance, respectively). The relations among these parameters are given by the following (Appendix 2):

$$J = q(1-r) , \tag{3.2}$$

$$h = \alpha . \tag{3.3}$$

The parameter q denotes the ratio of the average membrane potentials induced by the excitatory connections to the average total membrane potentials: $q = (\zeta_{SP}^{AV} + \zeta_{ex}^{AV})/|\zeta^{AV}|$.

At this stage, the interaction function $U_{j,j'}$ is modeled by the use of the Gaussian functions as follows:

$$U_{j,j'} = \frac{q_{ex}}{2\pi\lambda_{ex}^2}\exp\left(-\frac{d_{j,j'}^2}{2\lambda_{ex}^2}\right) - \frac{q_{inh}}{2\pi\lambda_{inh}^2}\exp\left(-\frac{d_{j,j'}^2}{2\lambda_{inh}^2}\right), \tag{3.4}$$

where $d_{j,j'}$ is the distance between j and j'. λ_{ex} and λ_{inh} are determined by the extent of excitatory and inhibitory lateral connections, respectively. q_{ex} and q_{inh} are proportional to the membrane potentials induced by excitatory and inhibitory neurons.

The spatial dependence of this interaction function is depicted in Fig. 1. General tendencies in ODC formation are not strongly dependent upon the detailed form of the interaction function. The important feature of the function is its short-range excitatory and long-range inhibitory behavior.

In addition to the parameters r and α introduced above, we here define another parameter κ by

$$\kappa = \frac{q_{inh}}{q_{ex}} , \tag{3.5}$$

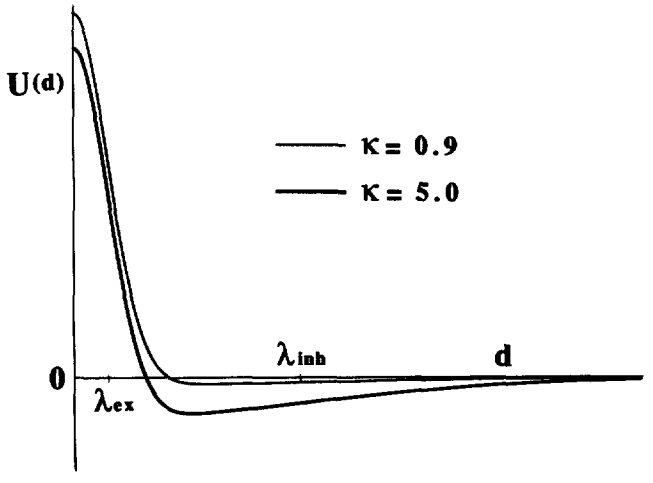

Fig. 1. Interaction functions. Two interaction functions used in computer simulations are shown for $\kappa = 5.0$ and 0.9 when $\lambda_{ex} = 0.15$, $\lambda_{inh} = 1.0$, and $q_{ex} = 1.0$. Here $q_{inh} = \kappa q_{ex}$

which stands for the ratio of membrane potentials induced by the inhibitory and excitatory neurons. This κ will be useful in analyzing segregated patterns.

4 Computer simulations

Since our mathematical theory is built on the statistical thermodynamics in the spin system, we can use the Monte Carlo computer simulation technique (Metropolis et al. 1953). This method describes the stochastic evolution of the spin configuration. In general, the spin configuration is updated if a random value between 0 and 1 generated by the computer is smaller than the transition probability. Otherwise, the configuration remains unchanged. In this simulation, we confine ourselves to the scheme of the single spin update per Monte Carlo step. The transition probability is given by

$$w(s_j \to -s_j) = \frac{1}{1+\exp\left(\frac{\Delta E_j}{T}\right)} , \tag{4.1}$$

where T is the effective temperature defined by (A1.3). ΔE_j is the energy difference between two spin configurations; one is the present configuration specified by s_j and the other is the configuration specified by $-s_j$ which would be taken at the next step. This energy difference is obtained from (3.1), that is,

$$\Delta E_j = -2\left(h + J\sum_{j'} U_{j,j'}s_{j'}\right)s_j . \tag{4.2}$$

Hereafter, we use the parameter β defined by $\beta = q/2T$. With the use of β, $\Delta E_j/T$ which determines the spin configuration through the transition probability given by (4.1) can be written as

$$\Delta E_j/T = -2\beta\left[\frac{\alpha}{q} + (1-r)\sum_{j'} U_{j,j'}s_{j'}\right]s_j . \tag{4.3}$$

If there is no imbalanced activity ($\alpha/q = 0$) in (4.3), it is found that ODC pattern formation is regulated by $\beta(1-r)$.

In the simulation, we use square panels which consist of 80×80 pixels. Each pixel corresponds to a small cortical area to which the value of the Ising spin variable is assigned according to the ocular dominance. Moreover, we impose a free boundary condition in the vertical direction and a periodic boundary condition in the horizontal direction.

5 Results

5.1 Effect of temperature and correlation strength

In the subsequent analysis by Monte Carlo simulations, we fix the parameter values as follows: $q_{ex} = 1.0$, $\lambda_{ex} = 0.15$, $\lambda_{inh} = 1.0$. The value of a (the edge length of one pixel) is selected such that the number of ocular dominance bands is 10 in the square panel. From the fact that the ODC period is about 0.8 mm for the macaque monkey (Hubel and Wiesel 1977), a corre-

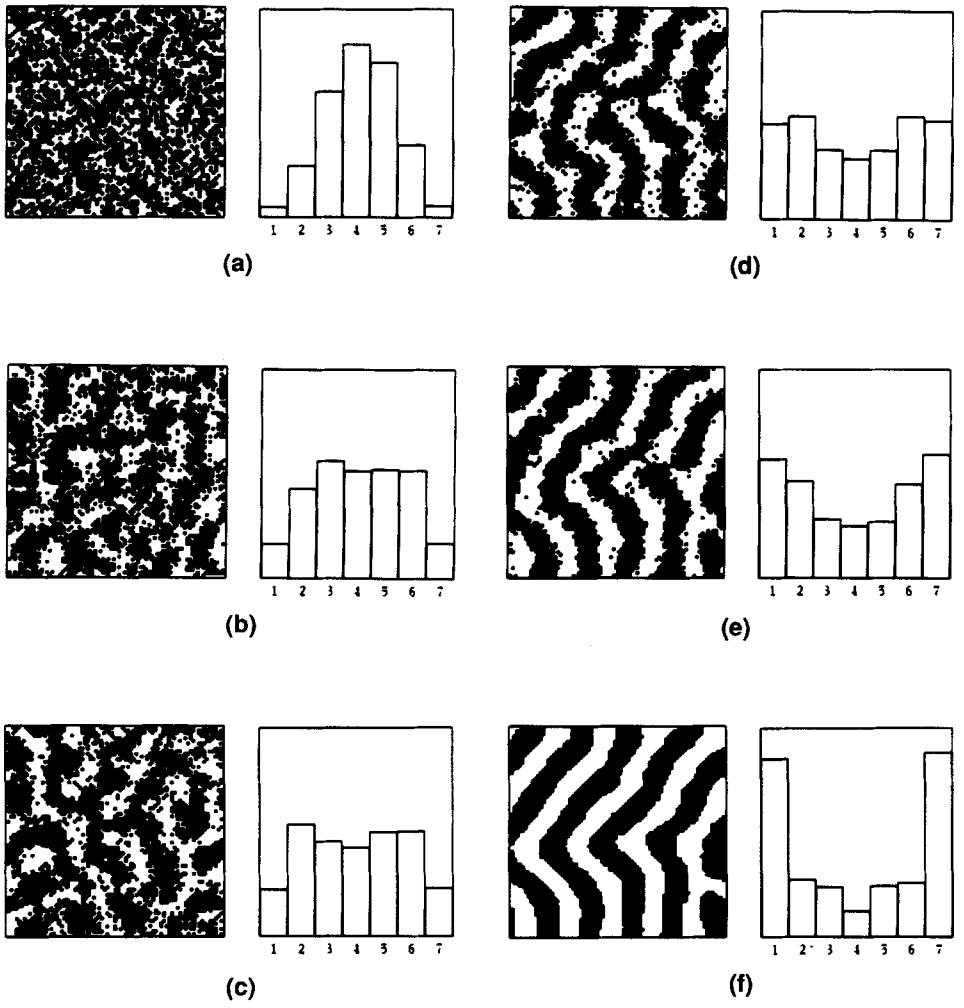

Fig. 2a–f. Computer-simulated ocular dominance patterns and corresponding ocular dominance histograms. These were obtained with large lateral inhibition ($\kappa = 5.0$) and balanced activities ($\alpha = 0$). The value of a is chosen as 0.118. Therefore, λ_{inh} and λ_{ex} amount to about 850 μm and 130 μm, respectively. While β is gradually increased from 1.0 in **a** to 1.6 in **b**, to 1.8 in **c**, to 2.2 in **d**, to 2.5 in **e**, and to 10.0 in **f**, the correlation strength r is fixed at 0. These patterns are also obtained when r is varied to 0.90, 0.84, 0.82, 0.78, 0.75, and 0.00, respectively, while β is fixed at 10.0 (see (3.10)). Ocular dominance is divided into 7 groups. If a neuron responds specifically to stimulus to the contralateral retina, it falls into group 1. If it responds only to stimulus to the ipsilateral retina, it falls into group 7. The neuron in group 4 responds to stimuli to both retinas with equal strength

sponds to 100 μm. Therefore, the actual values of λ_{inh} and λ_{ex} are given by 100 μm/a and 15 μm/a, respectively.

The computer simulations show that the stripe patterns become more segregated as β gradually increases (Figs. 2 and 3). The obtained stripe pattern is likely to be straight even though the existence of the anisotropic interaction function has not been assumed. It is observed that the ocular dominance histogram changes from a single-peak shape to a U-shape as the pattern segregates. Even though the value of β is fixed, we can also see stripe patterns segregate as the value of r decreases, since $\beta(1 - r)$ regulates pattern segregation, as noted before. When r decreases from 1 to zero, a stripe pattern starts segregating at a certain value of r. At this stage, the bandwidth is not constant and the border between ipsilateral-dominant and contralateral-dominant bands fluctuates. The pattern becomes sharper as r is further decreased. Finally we obtain the ODC stripe pattern with very sharp delimitations.

It is known that ODC segregation starts before birth (Rakic 1977). This means that form vision is not always necessary for ODC formation and that only spontaneous firing in RGCs is sufficient. We can explain this physiological observation by setting $r = 0$, which corresponds to no correlation between firings from the left and right retinas.

5.2 Straightness of stripe patterns

We can always see the stripes running in the vertical direction whenever we impose the free boundary condition on the horizontal boundaries and the periodic boundary condition on the vertical boundaries. This phenomenon observed in this simulation reflects the fact that the free boundary condition introduces anisotropy to the interaction function near the horizontal edges of the panel, while the periodic boundary condition does not distort the interaction function.

When κ is large, that is, inhibitory connections are more effective than excitatory ones, the pattern is likely to be straight. In contrast, if κ is small, the pattern is likely to be twisted or bent and to include branches and ends (compare Fig. 2f with Fig. 3f). When the pattern in Fig. 2f ($\kappa = 5.0$) is compared with the well-known experimental evidence (Hubel and Wiesel 1977), the similarity is striking. As a result, we can expect the lateral inhibition to be very effective in a biological system.

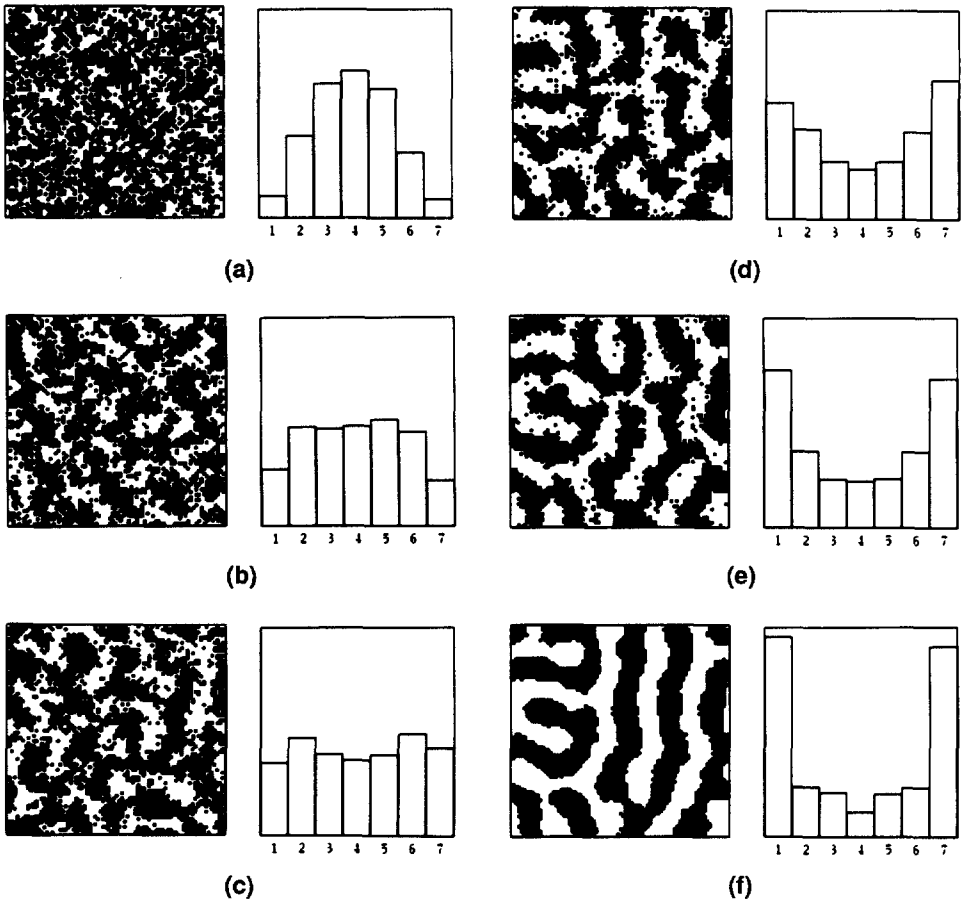

Fig. 3a–f. Computer-simulated ocular dominance patterns and corresponding ocular dominance histograms. These were obtained with small lateral inhibition ($\kappa = 0.9$) and balanced activities ($\alpha = 0$). a is chosen as 0.143. Therefore λ_{inh} and λ_{ex} amount to about 700 μm and 100 μm, respectively. While β is gradually increased from 1.0 in **a**, to 1.6 in **b**, to 1.8 in **c**, to 2.2 in **d**, to 2.5 in **e**, and to 6.0 in **f**, the correlation strength is fixed at 0. These patterns are also obtained by $r = 0.90$, 0.84, 0.82, 0.78, 0.75, and 0.40, respectively, for $\beta = 10.0$

The degree of the straightness also strongly depends on the rate of temperature decrease. Even if the value of κ is the same for the two given patterns, the gradually segregated ODC pattern is straighter (Fig. 2f) than the rapidly segregated one (Fig. 4). Moreover, we can see that the histogram given by the annealing technique shows a larger population of monocular neurons than that for rapid segregation. From the above discussions, we find that the straightness of the stripe pattern is controlled by the relative strength of lateral inhibition κ and the rate of temperature decrease.

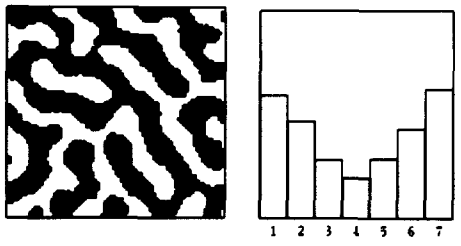

Fig. 4. A computer-simulated ocular dominance pattern and corresponding ocular dominance histogram. These were obtained with large lateral inhibition ($\kappa = 5.0$), balanced activities ($\alpha = 0$), and fixed correlation strength ($r = 0$). Note that β is suddenly changed from $\beta = 1.0$ to $\beta = 10.0$ so that the resulting pattern is not a straight parallel stripe as in Fig. 2f obtained with gradual increase of β

The ocular dominance histogram of the normal monkey has a dip at the 4th bin in the center of ocular dominance. We cannot see such a trend in the histogram under any conditions in the computer simulations. It can be inferred that this discrepancy is attributed to the approximation that the retinotopic order is achieved before ODC segregation starts. In fact, the results of computer simulations in which retinotopic map formation is taken into account in addition to ODC formation reproduce ocular dominance histograms similar to the experimentally obtained histogram (Tanaka 1990b).

5.3 Effect of the imbalance activity

It was reported that bandwidths are asymmetric between ipsilateral and contralateral bands in monocularly deprived animals. The wider bands observed in the experiment correspond to the regions where open-eye terminals project (Hubel et al. 1977). In our simulations, the situation for $\alpha \neq 0$ represents the presence of the bias in ocular dominance. We can again observe a good agreement between this experimental observation and our simulated results of asymmetric stripe patterns (the left column of patterns in Fig. 5).

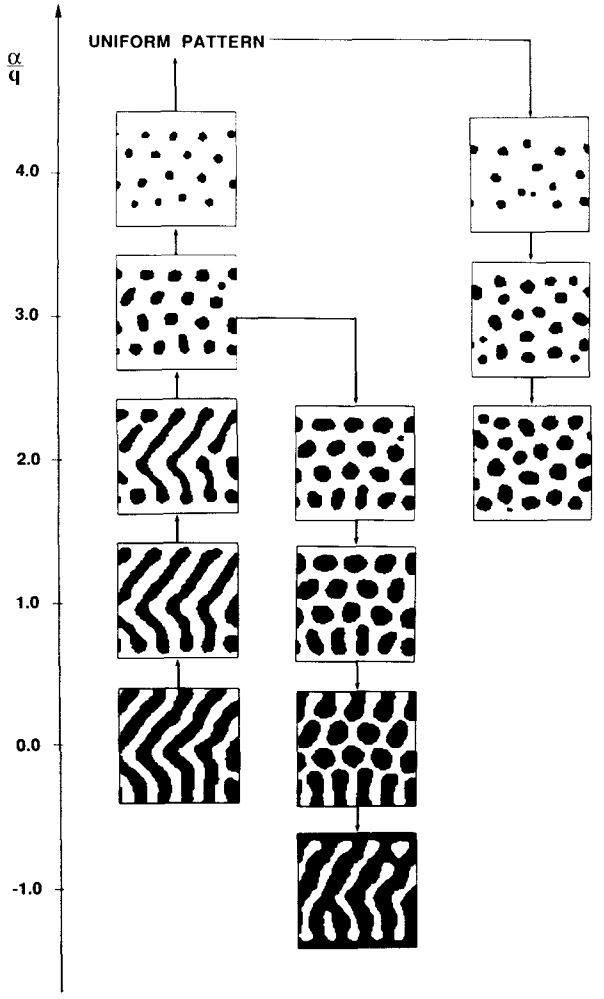

Fig. 5. Computer-simulated ocular dominance patterns for various imbalanced activities. Parameter values are as follows: $r = 0.0$, $\beta = 10.0$, $\kappa = 5.0$. The vertical axis gives the value of α/q. Arrows show the directions in which α/q is changed in the simulations. Note a kind of hysteresis; the emerging patterns depend upon the preceeding sequence of patterns. Therefore, two different patterns, the blob and stripe, are obtained even at the same $\alpha/q = 1.0$ since their initial patterns are different. An asymmetric stripe pattern remains during the increase from 0 to a large α/q value. But on the way back, a blob-lattice pattern is maintained up to a small α/q value

It was also reported that blob patterns have been observed in the region of the monkey primary visual cortex corresponding to the periphery in the visual field (LeVay et al. 1985). The blob pattern appears between the binocular region around a fovea and the monocular region far from the fovea. Our simulations show that the blob lattice patterns can emerge for $\alpha \neq 0$, in addition to the asymmetric stripe patterns. Here again, the experimental observation supports our theory. Furthermore, if the parameter value of q can be appropriately manipulated under monocular deprivation, it may be possible to observe the blob ODC pattern.

In natural phenomena, we often observe hysteresis which means the dependence of the state of a system on the previous history. Interestingly, a similar phenomena can be seen where the appearance of patterns depends upon the path along which the control parameter α/q moves. In practice, there can be two types of patterns at the same value of α/q: the stripe pattern and the blob pattern (compare the left and middle columns of patterns for $\alpha/q = 1.0$ and 2.0 in Fig. 5). For $\alpha/q > 5.0$, we obtain a uniform pattern with no deprived-eye-dominant synaptic terminals. The transition between this uniform pattern and the blob pattern seems to have no hysteresis (compare the left and right columns of patterns in Fig. 5).

6 Discussion and conclusion

In this report, a theory of ODC formation was built on the basis of our general theory of activity-dependent self-organization of cortical maps. From qualitative comparisons of computer simulation results with experimental observations, it was found that excellent agreement was achieved in various aspects of ODC formation. It was shown that three types of ODC patterns could be reproduced: stripe, blob, and uniform patterns. Their appearances are determined by the correlation strength and the degree of imbalance in activity between the left and right retinas.

We found that the spatially modulated patterns were more clearly segregated in the case of weaker correlation in activity between the left and right retinas. This can be understood in the following way. It is natural to think that the segregation of ODC patterns requires discrimination between two kinds of nerve terminals from the left and right retinas. The similarity between two firing patterns can be expressed by the correlation strength between the two. When electrical activities from the left and right retinas passing through the dorsal lateral geniculate nucleus (dLGN) transmit to the target dendrites, the target neurons cannot distinguish between the nerve terminals from the left and right retinas if the correlation between activities from both retinas is strong. Therefore, there is little or no segregation. On the other hand, the target neurons can clearly distinguish the terminals if the correlation is weak. In this case, there is clear segregation. As a result, we can say that the local Hebbian mechanism provides the correlation function which reflects the similarity between firing patterns at different synaptic terminals.

The strong lateral inhibition ($\kappa > 1$) was assumed in the simulations in which the straight parallel stripes were observed. This assumption implies the possibility of hyperpolarized membrane potentials in cortical neurons. For the neurons to elicit spike activities, either or both of the following two requirements should be satisfied: additional input activities originating in the region other than the dLGN elevate the membrane potentials and thereby facilitate firings of the neurons or most of cortical inhibitions are shunting inhibitions and therefore hyperpolarization is not so strong.

In our simulations, the annealing procedure in addition to the strong lateral inhibition was necessary to

obtain the straight parallel stripes. This may be partly attributed to the property of the interaction function used here. If we choose an adequate interaction function, the annealing procedure may not be necessary for the straight parallel stripe pattern segregation. In fact, the author confirmed that such stripe patterns were more easily segregated by carrying out the same simulations with the stepwise interaction function (Tanaka, in preparation). However, another interpretation is that annealing is actually performed in developing animals. This may be called developmental annealing in contrast to simulated annealing which is used as a general technique for obtaining the global minimum (Kirkpatric et al. 1983). As noted in Sect. 2, there is a close relationship between the presynaptic factor and the effective temperature. As the amount of the presynaptic factor decreases, the temperature drops. Therefore, developmental annealing actually occurs if the amount of the factor gradually decreases during the critical period.

In the theoretical formulation of our theory, the synaptic connection density was expressed by the spin variable which takes discrete values. This expression is justified by a winner-take-all process due to the competition among synapses for the limited amount of the postsynaptic factor. Because of this spin expression, we can successfully escape from introducing the additional constraints in other models of activity-dependent self-organization of neural networks (Von der Malsburg 1979; Miller et al. 1989; Linsker 1986). The exclusion of the additional constraints will make further development of our theory easier.

In addition, our theory has another unique feature in that it is built on the thermodynamics in the spin system, not on the deterministic time-evolutional equation for synaptic strength as in the model of Miller et al. (1989). The thermodynamic formulation makes a systematic analysis of cortical map self-organization possible, since the established mathematical procedures are available. Our general theory takes into consideration the fluctuation in the synaptic stabilization during development, which can be introduced as a finite temperature effect.

A detailed thermodynamic analysis will be given in a forthcoming paper (Tanaka, in preparation) in which the phase transition phenomenon in ODC formation will be discussed.

Acknowledgements. The author thanks Masao Ito, MD. and Dr. Tetsuya Takahashi of the Laboratory for Neural Networks, RIKEN Frontier Research Program, for useful advice and comments on this manuscript.

Appendix 1: mathematical background

Based on the mechanisms postulated in Sect. 2, the author proposed a basic dynamic equation which describes synaptic stabilization in the afferent nerve terminals depending on neuronal activity (Tanaka 1990a).

The following approximations were applied to this basic equation in order to derive a general framework within which cortical map self-organization is mathematically easier to deal with. First, firing of neurons in the presynaptic layer was assumed to be a stochastic process which is specified by the spatial correlation function $\Gamma_{k,\mu;k',\mu'}$. The subscripts k and k' represent the positions of two neurons in the presynaptic layer, while μ and μ' stand for types of pathways, such as ipsilateral or contralateral, on-center-off-surround or off-center-on-surround, and color specific or color non-specific, for the visual pathway. Second, the adiabatic approximation was employed since the time course for the electrical activity is thought to be much shorter than the time course for the synaptic stabilization process.

These approximations lead to a nonlinear stochastic differential equation for the connection density, which describes a winner-take-all process of synapses within a small region in the target layer. The area of this small region is determined by the diffusion length of the postsynaptic factor, since synapses compete strongly with one another in this region.

From the detailed mathematical discussion on local and global stability of solutions to the basic equation (Tanaka 1990a), we find that the equilibrium synaptic connection density $\rho_{j,k,\mu}$ can be expressed in terms of the total synaptic connection density ρ_{tot} and a variable $\sigma_{j,k,\mu}$ as follows:

$$\rho_{j,k,\mu} = \rho_{\text{tot}} \cdot \sigma_{j,k,\mu}, \tag{A1.1}$$

where if the neuron specified by k and μ in the presynaptic layer sends the axon to position j in the target layer, $\sigma_{j,k,\mu} = 1$, and if not, $\sigma_{j,k,\mu} = 0$. That is, the value of this variable for only one combination of k and μ for any j is 1 and the others are 0. These properties are the same as those for the Potts spin variable (Wu 1982). Thus, we can look upon the equilibrium solution of the equation as a set of Potts spin variables. As discussed previously (Tanaka 1990a), the problem can be reduced to the thermodynamics in the Potts spin system. Namely, the equilibrium behavior of the modifiable nerve terminals can be described in terms of the thermodynamics in this spin system in which the Hamiltonian H and effective temperature T are given by

$$H = -\text{sgn}(\zeta^{AV}) \sum_{j,\mu} \sum_{k \in B_{j,\mu}} \varphi_{k,\mu} \sigma_{j,k,\mu} - q \sum_{\substack{j,\mu \\ j',\mu'}} \sum_{\substack{k \in B_{j,\mu} \\ k' \in B_{j',\mu'}}} V_{j,j'} \Gamma_{k,\mu;k',\mu'} \sigma_{j,k,\mu} \sigma_{j',k',\mu'}, \tag{A1.2}$$

$$T = \frac{\sqrt{\pi}}{2} \gamma \sqrt{\frac{\tau_c}{\tau_s}}, \tag{A1.3}$$

where $\varphi_{k,\mu}$ in the first term of (A1.2) is the averaged firing frequency which is normalized such that the value is of the order of 1, and γ is a rough estimate for the ratio of the standard deviation of the firing frequency to the averaged firing frequency. $V_{j,j'}$ describes the interaction between synapses in the target layer. $\mathbf{B}_{j,\mu}$ is a set of possible neurons specified by the neuronal type μ which send axonal terminals to position j in the target layer (Tanaka 1990a). q is the ratio of the averaged

membrane potential induced through the modifiable synapses ζ_{SP}^{AV} to the absolute value of the total averaged membrane potential $|\zeta^{AV}|$. That is,

$$q = \frac{\zeta_{SP}^{AV}}{|\zeta^{AV}|}. \tag{A1.4}$$

$\Gamma_{k,\mu;k',\mu'}$ represents the normalized correlation strength between the firings elicited from two cell bodies which are specified by (k, μ) and (k', μ'). τ_c is the correlation time of the electrical activities and τ_s is the time course for the synaptic stabilization process.

In this theory, the type of pattern segregated from a uniform structure is mainly determined by the correlation function. This function is determined by the statistical properties of neural activity in the modality and/or submodality.

Appendix 2: reduction to the Ising spin system

In order to obtain an appropriate Hamiltonian describing ODC formation, the correlation function and related parameters should be determined.

In deriving the function which describes the correlation between firing frequencies from RGC in the left retina and in the right retina, it is assumed that the dLGN plays only the role of a relay nucleus which transmits neural activity from RGCs to the primary visual cortex without any additional information processing.

We can obtain an appropriate mathematical description for the correlation function of RGC activity, by considering the following presumptions: *(i)* there are two types of firings, spontaneous and visually stimulated, which are stochastically independent of each other; *(ii)* the spontaneous firing in one retina does not correlate with that in the other retina, since the two firings are spatially separated; *(iii)* the visually stimulated firings in both retinas can be correlated if the two firings occur at retinotopically corresponding positions, since the same light stimulus falls on these two positions; and *(iv)* spatial correlation between two distant RGCs within a single retina may be realized by mutual horizontal connections due to horizontal cells and amacrine cells; *(v)* finally, the property of the spatial correlation for the spontaneous firings within one retina is assumed to be the same as that for the visually stimulated firings.

From the presumptions concerning properties of the correlation function of RGC activity, we obtain a mathematical form of the correlation function:

$$\Gamma_{k,\mu;k',\mu'} = \frac{1}{\bar{\eta}^2}(\xi_\mu^V \xi_{\mu'}^V + \xi_\mu^S \xi_{\mu'}^S \delta_{\mu,\mu'}) C_{k,k'}, \tag{A2.1}$$

where ξ^V and ξ^S are the standard deviations of the visually stimulated firing frequency and that of the spontaneous firing frequency, respectively. $\delta_{\mu,\mu'}$ is Kronecker's delta. The spatial correlation is represented by $C_{k,k'}$.

Now we define a parameter which describes the correlation of firings elicited from the left and right RGCs as follows:

$$r = \frac{\xi_{+1}^V \xi_{-1}^V}{\xi_{+1} \xi_{-1}}, \tag{A2.2}$$

where $\xi_\mu = \sqrt{(\xi_\mu^V)^2 + (\xi_\mu^S)^2}$. If there are only spontaneous firings ($\xi_\mu^V = 0$), there is no correlation between the left and right RGC firings ($r = 0$). On the other hand, in the presence of visual stimulation, firings from the left and right retinas correlate ($0 < r \leqslant 1$), since, in normal animals, the two RGCs which have retinotopic correspondence to each other on the respective retinas receive almost the same images. For simplicity, it is assumed that $\xi_{+1} = \xi_{-1} = \gamma\bar{\eta}$.

Next, let $\bar{\varphi}_{+1}$ and $\bar{\varphi}_{-1}$ denote the normalized average firing frequencies of ipsilateral and contralateral RGCs. Using these we can define another important parameter α as follows:

$$\alpha = \frac{\bar{\varphi}_{+1} - \bar{\varphi}_{-1}}{\bar{\varphi}_{+1} + \bar{\varphi}_{-1}}. \tag{A2.3}$$

α stands for the degree of imbalance in firing activity between the left and right RGCs.

We adopt the following factorization in order to separate ocular dominance and retinotopic order:

$$\sigma_{j,k,\mu} = \sigma_{j,k}^R \sigma_{j,\mu}^{OD}. \tag{A2.4}$$

where $\sigma_{j,k}^R$ and $\sigma_{j,\mu}^{OD}$ are the Potts spin variable for retinotopic order and that for ocular dominance, respectively.

The ocular dominance in anatomical connections to position j in the visual cortex can be specified by the Ising spin defined by

$$s_j = \sum_{k,\mu} \mu \sigma_{j,k,\mu}. \tag{A2.5}$$

s_j takes only $+1$ or -1, according to ipsilateral or contralateral dominance. Since $\sum_k \sigma_{j,k}^R = 1$, it is also represented as follows:

$$s_j = \sum_{\mu = +1,-1} \mu \sigma_{j,\mu}^{OD}, \tag{A2.6}$$

By the use of this Ising spin variable, the Hamiltonian of this system can be reduced to

$$H = -\sum_j h_j s_j - \frac{J}{2} \sum_{j \neq j'} \sum_{j'} U_{j,j'} s_j s_{j'}, \tag{A2.7}$$

where terms independent of the spin variables are omitted since they are irrelevant to ODC formation. h_j stands for the external bias applied to s_j, while $U_{j,j'}$ is the interaction between two Ising spins, s_j and $s_{j'}$. That is, the first term of (A2.7) reflects the ocular dominance shift, while the second term is essential to ODC segregation. h_j and $U_{j,j'}$ include the effect of retinotopic order as follows:

$$h_j = \tfrac{1}{2} \operatorname{sgn}(\zeta^{AV}) \sum_{\mu,k} \mu \varphi_{k,\mu} \sigma_{j,k}^R, \tag{A2.8}$$

$$U_{j,j'} = \gamma^2 V_{j,j'} \sum_{k \in B_j} \sum_{k' \in B_{j'}} C_{k,k'} \sigma^R_{j,k} \sigma^R_{j,k'} . \quad \text{(A2.9)}$$

J in (A2.7) can be expressed in terms of r:

$$J = q(1-r) . \quad \text{(A2.10)}$$

If $\sum_k \varphi_{k,\mu} \sigma^R_{j,k}$ is weakly dependent upon j, it turns out to be the normalized average firing frequency $\bar{\varphi}_\mu$ which satisfies $\bar{\varphi}_{+1} + \bar{\varphi}_{-1} = 2$. In this case, h_j is reduced to a constant h independent of j. It is written by the use of α as follows:

$$h = \alpha \cdot \mathrm{sgn}(\zeta^{AV}) . \quad \text{(A2.11)}$$

As can be seen from (A2.11), the external bias represented by the first term of the reduced Hamiltonian (A2.7) takes the same sign as α does when the cell membranes of the cortical neurons are, on the average, depolarized ($\zeta^{AV} > 0$). On the other hand, it takes the opposite sign when the membranes are hyperpolarized ($\zeta^{AV} < 0$). In this paper, only the case for $\zeta^{AV} > 0$ was discussed.

There can be two types of excitatory interactions between synapses. One is the interaction between synapses attached to the dendrites of the same neuron. The other is the interaction between synapses attached to the dendrites of different neurons via the lateral axonal connection between these neurons. The first term in (3.4) includes these two types of the excitatory interactions. Because of this unification of the interactions, the parameter q seen in (3.2) and (A2.10) should be defined by $q = (\zeta^{AV}_{SP} + \zeta^{AV}_{ex})/|\zeta^{AV}|$. Therefore, the definition of q is different from that in (A1.4), $q = \zeta^{AV}_{SP}/|\zeta^{AV}|$.

Appendix 3: occular dominance distribution

It is convenient to introduce "ocular dominance distribution" which represents the distribution of neurons to ocular dominance in their response to monocular light stimuli. Hubel and Wiesel (1962) used the so-called ocular dominance histogram in which ocular dominance is divided into 7 bins in the horizontal axis. For the purpose of introduction of such distribution functions, we define the degree of ocular dominance for the response of the nth neuron at position j_n, O_n, by

$$O_n = \eta_{j_n}(\mu = +1) - \eta_{j_n}(\mu = -1)$$
$$= F_\theta(\zeta_{j_n}(\mu = +1)) - F_\theta(\zeta_{j_n}(\mu = -1)) , \quad \text{(A3.1)}$$

where $\eta_{j_n}(\mu = +1)$ or $\eta_{j_n}(\mu = -1)$ means the firing frequency of the neuron at position j_n when the light stimulus is presented to either the ipsilateral or contralateral retina. F_θ is the nonlinear transformation function from the membrane potential to the firing frequency with the threshold potential θ. If the membrane potential at the cell body becomes larger than the value of θ, the neuron fires.

Next, we use the same approximation for the firings in the cortical neurons, as in the previous paper (Tanaka 1990a), in deriving the general Hamiltonian. Then we obtain the following formula:

$$O_n \cong (\zeta_{j_n}(\mu = +1) - \zeta_{j_n}(\mu = -1)) h(\zeta - \theta)$$
$$= h(\zeta - \theta) \sum_{j',k,\mu} V_{j_n,j'} \mu \sigma_{j',k,\mu} \eta_{k,\mu}$$
$$\cong \bar{\eta} h(\zeta - \theta) \sum_{j'} V_{j_n,j'} s_{j'} . \quad \text{(A3.2)}$$

$h(\zeta - \theta)$ can be expressed by the integration of the error function (Tanaka 1990a). We can calculate the degree of ocular dominance related to neuronal response by using the last equation in (A3.2) and the Ising spin which represents anatomical ocular dominance.

Ocular dominance distribution $D(\varepsilon)$ is defined by

$$D(\varepsilon) = \frac{1}{N} \sum_n^N \delta\left(\varepsilon - \frac{O_n}{O_{\max}}\right), \quad \text{(A3.3)}$$

where N stands for the number of sampled neurons, δ is Dirac's delta function, and $O_{\max}$ is the maximum value of all the O_n's. $\varepsilon = 0$ means a complete binocular response. $\varepsilon = +1$ and -1 corresponds to completely ipsilateral dominance and contralateral dominance, respectively. It is straightforward to rewrite (A3.3) in the form of the ocular dominance histogram. Ocular dominance is divided into 7 groups according to the definition by Hubel and Wiesel (1962). If a neuron responds specifically to stimulus to the contralateral retina, it falls into group 1. If it responds only to stimulus to the ipsilateral retina, it falls into group 7. The neuron in group 4 responds to stimuli to both retinas with equal strength. Therefore, the response of neurons in groups 1 and 7 are monocular, and those in group 4 are binocular.

References

Changeux JP, Danchin A (1976) Selective stabilization of developing synapses as a mechanism for the specification of neuronal networks, Nature 264:705–712

Collingridge GL, Bliss TVP (1987) NMDA receptors – their role in long-term potentiation, Trends Neurosci 10:288–293

Frank E (1987) The influence of neuronal activity on patterns of synaptic connections. Trends Neurosci 10:188–190

Hubel DH, Wiesel TN (1962) Receptive fields, binocular interaction and functional architecture in the cat's visual cortex. J Physiol 160:106–154

Hubel DH, Wiesel TN (1977) Functional architecture of macaque monkey visual cortex. Proc R Soc Lond B198:1–59

Hubel DH, Wiesel TN, LeVay S (1977) Plasticity of ocular dominance columns in monkey striate cortex. Phil Trans R Soc Lond B278:377–409

Hubel DH, Wiesel TN, Stryker MP (1978) Anatomical demonstration of orientation columns in macaque monkey. J Comp Neurol 177:361–380

Kaas JH, Merzenich MM, Killackey HP (1983) The organization of somatosensory cortex following peripheral nerve damage in adult and developing mammals. Ann Rev Neurosci 6:325–356

Kirkpatric S, Gellat CD, Vecchi MP (1983) Optimization by simulated annealing. Science 220:671–680

Knudsen EI, DuLac S, Esterly SD (1987) Computational maps in the brain. Ann Rev Neurosci 10:41–65

LeVay S, Connolly M, Houde J, Van Essen DC (1985) The complete pattern of ocular dominance stripes in the striate cortex and visual field of the macaque monkey. J Neurosci 5:486–501

Linsker R (1986) From basic network principles to neural architecture: Emergence of spatial-opponent cells. Proc Natl Acad Sci USA 83:7508–7512
Livingstone MS, Hubel DH (1984) Anatomy and physiology of a colorsystem in the primate visual cortex. J Neurosci 4:309–356
Metropolis N, Rosenbluth AW, Rosenbluth MN, Teller AH, Teller E (1953) Equation of state calculations by fast computing machines. J Chem Phys 21:1087–1092
Miller KD, Keller JB, Stryker MP (1989) Ocular dominance column development: analysis and simulation. Science 245:605–615
Rakic P (1977) Prenatal development of the visual system in Rhesus monkey. Phil Trans R Soc Lond B278:245–260
Swindale NV (1980) A model for the formation of ocular dominance stripes. Proc R Soc Lond B208:243–264
Tanaka S (1988) Theory of self-organization of cortical maps. In: The proceeding of SICE '88, ESS2-5:1069–1072
Tanaka S (1989) Theory of self-organization of cortical maps. In: Touretzky DS (ed) Advances in neural information processing system, Vol 1. Morgan Kaufmann, San Mateo Calif, pp 451–458
Tanaka S (1990a) Theory of self-organization of cortical maps: mathematical framework. Neural Networks: (to be published)
Tanaka S (1990b) Experience-dependent self-organization of biological neural networks. NEC Res Dev 98:1–14
Von der Malsburg C (1979) Development of ocularity domains and growth behavior of axon terminals. Biol Cybern 32:49–62
Wu FY (1982) The Potts model. Rev Mod Phys 54:235–268

Dr. Shigeru Tanaka
Fundamental Research Laboratories
NEC Corporation
34 Miyukigaoka, Tsukuba
Ibaraki
305 Japan